Nonlinear Behavior of a Shim Coil in an LTS/HTS NMR Magnet With an HTS Insert Comprising Double-Pancake HTS-Tape Coils

Nonlinear Behavior of a Shim Coil in an LTS/HTS NMR Magnet With an HTS Insert Comprising Double-Pancake HTS-Tape Coils

Seung-yong Hahn, Min Cheol Ahn, Juan Bascuñán, Weijun Yao, and Yukikazu Iwasa

***Abstract*—This paper reports results, experimental and analytical, of the nonlinear behavior of a shim coil in the presence of an HTS coil assembled with double-pancake (DP) HTS-tape coils. The experimental results are from: 1) operation of a 700 MHz LTS/HTS NMR magnet (LH700) consisting of a 600 MHz LTS NMR magnet (L600) equipped with superconducting shim coils and a 100 MHz DP-assembled HTS insert (H100) and; 2) an experiment with a room-temperature (RT) $Z1$ shim coil coupled to a 50 MHz DP-assembled HTS insert (H50). A field mapping theory with a harmonic analysis is applied to interpret both results. Based on experimental results and analyses, we conclude that the screening-current-induced field (SCF) generated by a DP-assembled HTS insert is primarily responsible for the nonlinear behavior, including strength degradation, of a shim coil.**

***Index Terms*—Double-pancake coils, field homogeneity, HTS insert, LTS/HTS NMR magnet, nonlinear behavior of a shim coil, screening-current-induced field.**

I. Introduction

NUCLEAR magnetic resonance (NMR) phenomenon has been widely used in various applications including chemistry, medicine, and nondestructive testing of nucleic acids such as DNA and RNA or proteins. With the need to analyse more complicated structures of materials by NMR techniques increases, so is the need to increase the field of superconducting NMR magnets. Recently, a field of 22.3 T (corresponding to a 950 MHz ^{1}H NMR frequency), to-date the highest, was achieved with an all-LTS (low temperature superconductor) NMR magnets [1]. Despite incessant demands by NMR users for even higher fields, it is generally agreed that 1 GHz is a limit achievable with all-LTS NMR magnets, primarily because of low current-carrying capacities of LTS, even at 1.8 K, in fields above ~24 T. We believe that HTS (high temperature Superconductor) is the only superconductor that enables a magnet to surpass 1 GHz. Based on this belief we started in 2000 a 3-phase program with a final goal to complete a 1 GHz high-resolution LTS/HTS NMR magnet. Recently, we completed the 2nd phase, in which a 700 MHz LTS/HTS NMR magnet (LH700) was designed, constructed and tested; the LH700 consists of a 600 MHz LTS NMR magnet (L600), equipped with superconducting shim coils, and a 100 MHz HTS insert (H100) assembled with double-pancake (DP) coils wound with Bi2223 tape [2], [3].

When the L600 superconducting shim coils were energized, for the first time, in the test of LH700 at 692 MHz, we found a strong nonlinear behavior of the shim coils including below-spec performance, i.e. shim strength degradation. Specifically, a shimming field from each set was not linearly proportional to current nor did it reach its specified value, making it very difficult to shim out field impurities. In fact, the dominant field gradients—$Z1$, Y, and ZY—could not completely be removed for lack of enough shim strength [3].

This paper presents the nonlinear behavior of the L600 superconducting shim coils observed during the operation of LH700. Shimming results from LH700 were analysed with a field mapping theory [4]. Based on the results, experiment and analysis, it appeared that the screening-current-induced field (SCF) generated by the 100 MHz HTS insert was primarily responsible for the observed nonlinear behavior of the shim coils. To further study and quantify this nonlinear behavior of the L600 shim coils, a room-temperature (RT) $Z1$ shim coil was coupled to and tested with the 50-MHz HTS insert (H50) of the Phase 1 350 MHz LTS/HTS NMR magnet (LH350), completed in 2003 [5]. The performance of the $Z1$ RT shim coil is presented first, followed by its test results and discussion.

II. Shim Coil Performance in LH700

A. System Configuration of LH700

Fig. 1 shows a schematic drawing of the LH700 where eight shim coils up to the 2nd order ($Z1$, $Z2$, X, Y, ZX, ZY, $C2$, and $S2$) are installed radially outside the LTS background magnet, L600. Table I summarizes key magnet parameters of L600 and H100 including those eight shim coil strength values that were measured separately without the H100; maximum current allowed through each shim coil is 20 A, though, in the actual operation, we limited the shim coil current up to 18 A for safety. Note that the shim coils were designed and constructed to mitigate field impurity specifically from the L600 so that their strengths were not strong enough to completely remove those from the H100.

B. Degradation of Shim Coil Strength in LH700

In a field mapping of LH700, a ^{1}H NMR probe was helically traced over a cylindrical surface of 17 mm diameter and 30 mm long in 12 revolutions. Fig. 2 shows two field mapping results in

Manuscript received August 19, 2008. First published June 30, 2009; current version published July 15, 2009. This work was supported by the NIH National Center for Research Resources.

The authors are with the Francis Bitter Magnet Laboratory, Massachusetts Institute of Technology, Cambridge, MA 0213, USA (e-mail: syhahn@mit.edu; minchul@mit.edu; bascunan@mit.edu; wyao@mit.edu; iwasa@jokaku.mit.edu).

Color versions of one or more of the figures in this paper are available online at http://ieeexplore.ieee.org.

Digital Object Identifier 10.1109/TASC.2009.2018809

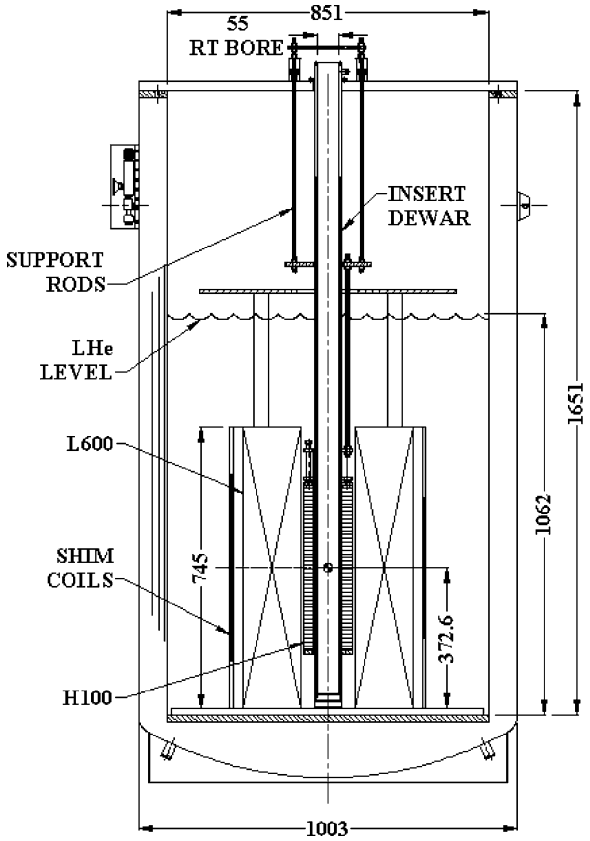

Fig. 1. To-scale schematic drawing of the LH700; all the shim coils are located radially outside the LTS magnet, L600.

TABLE I
MAGNET PARAMETERS AND SHIM COIL STRENGTH OF LH700

Parameters	H100	L600
Magnet parameters		
Overall i.d.; o.d. [mm]	78; 126.5	142; 826
Overall height [mm]	405.6	1246
Operating current [A]	116.0	234.9
Center field [T]	2.35	14.1
Inductance [H]	0.88	90
Shim coil strength		
$Z1$ [Hz/cm/A]	--	4025
$Z2$ [Hz/cm^2/A]	--	107
X, Y [Hz/cm/A]	--	1047
ZX, ZY [Hz/cm^2/A]	--	365
$C2$ (X^2-Y^2), $S2$ (XY) [Hz/cm^2/A]	--	115

full operation of LH700; Dashed line with a triangle represents a mapping taken before shimming while solid line with a circle after shimming with maximum currents, 18 A, of the $Z1$, Y, ZX, and ZY shim coils and 8 A of the X shim coil—$C2$ and $S2$ were not activated. Overall homogeneity within the cylindrical mapping volume was improved from 351 ppm to 172 ppm by shimming though it was still much larger than the target homogeneity of $\sim$3 ppm [5].

Table II summarizes three dominant field gradients—$Z1$, Y, and ZY—of the two mappings in Fig. 2; "Before" represents field gradients before shimming; "After" those after shimming; "Shim strength" was calculated by the difference between "Before" and "After" divided by the shim coil current, 18 A. Note that each shim strength in the actual operation was degraded

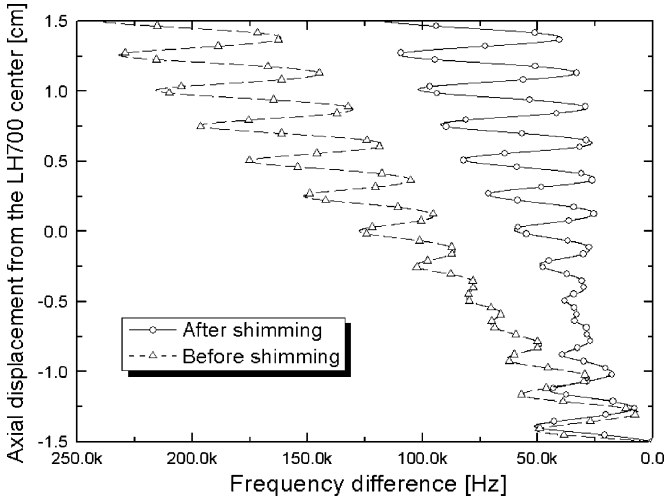

Fig. 2. Field mapping results of the LH700; dashed line with a triangle: before shimming; solid line with a circle: after shimming.

TABLE II
MAJOR FIELD GRADIENTS OF THE LH700 MEASURED BEFORE AND AFTER SHIMMING AND THEIR CORRESPONDING SHIM STRENGTHS

Field gradients	Before	After	Shim strength*
$Z1$ [Hz/cm]	63895	18009	2549
Y [Hz/cm]	20489	18927	86.8
ZY [Hz/cm^2]	31076	29242	102

* Units: $Z1$ and Y [Hz/cm/A], ZY [Hz/cm^2/A]

* Shim strength varied to operating conditions of each shim coil.

from those measured without the H100 in Table I; the tesseral shim strengths of Y and ZY were degraded more than the zonal shim strength of $Z1$ in percentage.

III. TEST OF A $Z1$ ROOM-TEMPERATURE SHIM COIL WITH H50

To further investigate the non-linear behavior of a shim coil in a stacked-DP type HTS insert wound with Bi2223 tapes, a Room-Temperature (RT) $Z1$ shim coil was designed, constructed, and tested with a 50 MHz HTS insert (H50) which was disassembled from the Phase 1 350 MHz LTS/HTS NMR magnet (LH350) completed in 2003 [6].

A. Test Set-Up and Procedure

Fig. 3 shows a schematic to-scale drawing of the RT $Z1$ shim coil coupled to the H50. The $Z1$ shim coil consists of two geometrically identical loops with opposite directions of operating current. An AWG-18 copper wire of 3.8 m long was used for each current loop to form a single layer with 10 turns and the calculated shim strength at the center of H50 was 1171 Hz/cm/A that corresponded to 0.275 gauss/cm/A. Key parameters of the $Z1$ RT shim coil are presented in Table III. During the test, axial field distribution along the axis of H50 was measured using a search coil moved by a speed-controllable DC step motor.

Test procedure is as follows; 1) The H50 and $Z1$ shim coil were placed in an LN_2 dewar without any cryogen at room-temperature and axial field distributions were measured at sequential shim coil currents of $0 \rightarrow 5 \rightarrow 0 \rightarrow -5$ A and $0 \rightarrow 1 \rightarrow 0 \rightarrow -1$ A; 2) The same two sets of tests were repeated while the H50 and $Z1$ shim coil were placed in a bath of LN_2 at 77 K. In the 77-K tests, the H50 and Z1 shim coils were completely

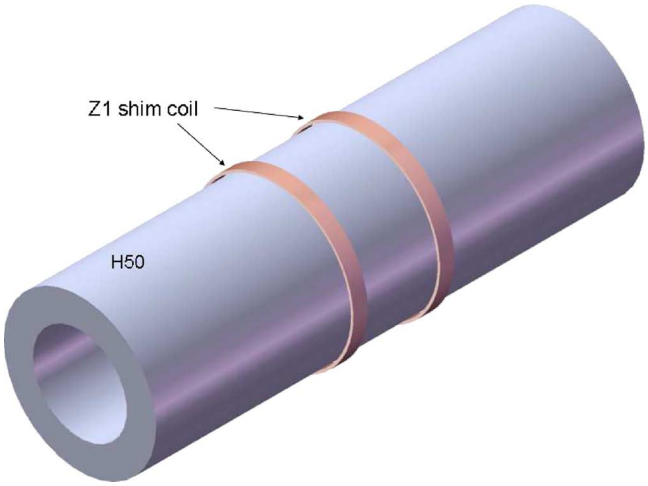

Fig. 3. Schematic to-scale drawing of the $Z1$ RT shim coil coupled to the H50.

TABLE III
KEY DESIGN PARAMETERS OF THE RT $Z1$ SHIM COIL

Parameters	RT Z1 shim coil
Material	Copper (AWG 18)
Overall i.d.; o.d. [mm]	121; 123
Height of a loop [mm]	12
Distance between two loops [mm]	60
Turns per layer; layer	10; 1
Total inductance [uH]	43.3
Total resistance [Ω]	0.1
Total wire length [m]	7.6
Shim strength [Hz/cm/A]	1171

warmed up to room-temperature between the 5-A and 1-A sets of tests to clear the previous charging history.

B. Performance of the $Z1$ RT Shim Coil

Fig. 4 presents axial field measurements at shim coil currents of a) ± 5 A and b) ± 1 A with two different temperatures of 300 K and 77 K, respectively, while the H50 was not energized; Solid triangle and solid square indicate the results at 300 K with positive and negative operating currents respectively; Open triangle and open square indicate those at 77 K. The measured $Z1$ shim strengths at the H50 center from the Fig. 4 are summarized in Table IV; The $Z1$ shim strengths at 300 K ranged from 1151 to 1218 Hz/cm, which is consistent with the design frequency, 1171 Hz/cm while those measured at 77 K varied more widely from 175 to 673 Hz/cm which were degraded by more than 40% from the design frequency. Note that the non-linear variation of the $Z1$ shim strength measured at 77 K was enhanced as the shim current was reduced ($5 \rightarrow 1$ A) because of a corresponding relative strength increase of the Screening Current induced Field (SCF) in the H50. This non-linear variation of the shim strength as well as its strength degradation made it very difficult to completely remove the dominant field gradients of the LH700 as seen in Fig. 2 and Table II. More research on the shim coil performance in the presence of an HTS coil will be required for a high-resolution LTS/HTS NMR magnet where a precise shimming is crucial.

TABLE IV
MEASURED AND DESIGNED Z1 RT SHIM STRENGTH VALUES

Parameters	Shim current			
	1 A	-1 A	5 A	-5 A
Measured				
300 K [Hz/cm/A]	1154	-1218	1151	-1183
77 K [Hz/cm/A]	175	-673	549	-661
Designed [Hz/cm/A]	1171	-1171	1171	-1171

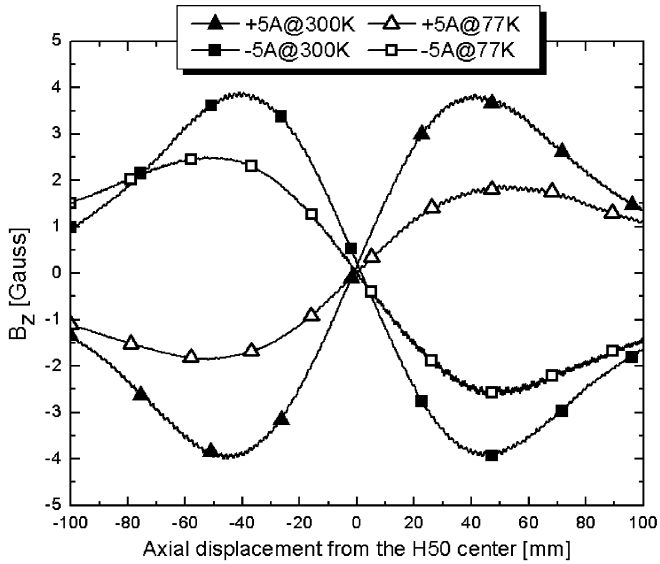

(a)

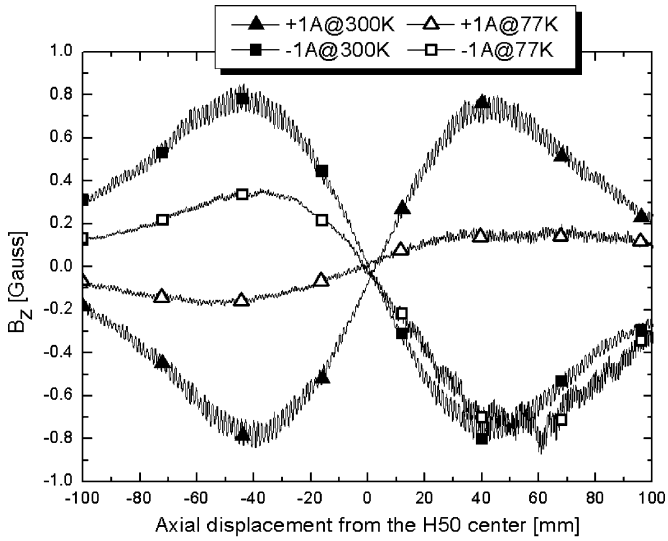

(b)

Fig. 4. Axial field distribution generated by the $Z1$ RT shim coil along the H50 axis operated at 300 K and 77 K with shim coil currents of: (a) ± 5 A; (b) ± 1 A.

C. Canceling a $Z1$ Gradient of SCF From the H50

In a bath of LN_2, we charged the H50 up to 15 A and then completely discharged it with the intention of generating an SCF in the bore of H50 and canceling the $Z1$ gradient of the SCF by the $Z1$ RT shim coil. Fig. 5 shows measured axial field, B_z, profiles along the H50 axis with different operating currents of the $Z1$ shim coil; The open squares represent a B_z distribution before the $Z1$ shim coil was activated; The solid circles are a

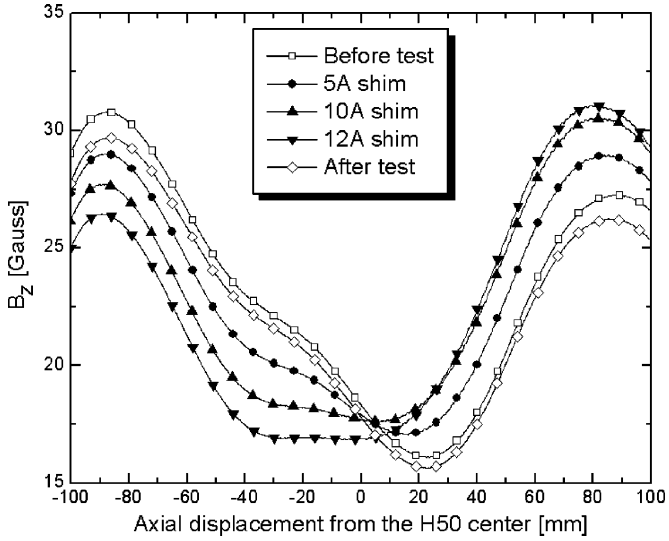

Fig. 5. Axial field distribution along the H50 axis with various $Z1$ shim coil currents after the SCF was induced in the H50.

TABLE V
ANALYSIS OF THE MEASURED Z1 GRADIENTS IN FIG. 5

Operating conditions	Measured Z1 [Hz/cm]	Shim strength [Hz/cm/A]
Before test	-6538	--
5 A	-3795	549
10 A	-1269	505
12 A	243	756
After test	-6921	--

5-A $Z1$ shim current applied; The solid triangles are a current of 10-A; The solid reverse triangles are with 12 A applied when the $Z1$ gradient at the H50 center was almost canceled out; The open diamonds indicate a B_z measured after the $Z1$ shim current returned to zero.

Table V summarizes the measured $Z1$ gradient at the H50 center in Fig. 5; the "Shim strength" was defined as the average variation of the $Z1$ gradient divided by the shim current variation at a given operating condition, e.g. that of "12 A", 756 Hz/cm/A, was obtained by $(243+1269)/2$. While the change of shim current was every 5 A ($0 \rightarrow 10$ A), the shim strengths were not changed much although they were still less than 50% of the measured one at 300 K in Table IV. However, when the change of shim current was 2 A ($10 \rightarrow 12$ A), its non-linearity increased similarly as seen in Fig. 4(b) because of a corresponding relative increase in the SCF strength.

In Fig. 5, the B_z measured after the shim current returned to zero, "After test", is different from that measured before the tests started, "Before test", because of a temporal instability of the SCF which is explained in detail in [7]. This may cause another problem in finding a frame of reference for shimming. In general, a frame of reference is obtained by subtracting two mappings with opposite currents of $Z1$, X, and Y shim coils. If the time-dependent SCF is added to the field from shim coils, it may be more difficult to find a frame of reference. Currently, we are devoting our efforts in better understanding the frame-of-reference related issues as well as non-linear behavior of shim coils in an LTS/HTS NMR magnet having a DP-type HTS magnet as an insert.

IV. CONCLUSION

Using a field mapping analysis, we have investigated the nonlinear behavior (and below-specs performance) of the L600 superconducting shim coils observed during operation of LH700. To further understand this nonlinear behavior of the L600 shim coils in the presence of H100, a room-temperature (RT) $Z1$ shim coil was coupled to and tested with H50. Based on our investigation, experimental and analytical, of both systems, we may conclude that:

- The primary reason that the dominant field gradients—$Z1$, Y, ZY—of LH700 could not be completely shimmed out is the nonlinear behavior of the L600 superconducting shim coils.
- The screening-current-induced field (SCF) generated by H100 is the primarily source responsible for this unexpected nonlinear behavior of the L600 shim coils.
- The nonlinear behavior as well as the degradation of a shim coil in the presence of a DP-assembled HTS insert was further confirmed by an experiment with a $Z1$ RT shim coil coupled to the H50.
- The nonlinearity of the $Z1$ RT shim coil increased as the field of the $Z1$ RT shim was reduced, apparently because of a corresponding relative increase in the SCF strength.
- A "time-dependent" SCF may compound the problem of shimming because it will be more difficult to find a frame of reference for shimming an LTS/HTS NMR magnet.
- Understanding the nonlinear behavior of a shim coil as well as the temporal and spatial characteristics of an SCF is critical to successfully construct an above 1 GHz *high-resolution* LTS/HTS NMR magnet, particularly if the magnet incorporates an HTS insert assembled with DP coils wound with HTS tapes. Specifically, a set of superconducting shim coils, to be placed in the LTS magnet of such an LTS/HTS NMR magnet, must be designed to mitigate or even eliminate the effects of this nonlinear behavior caused by the HTS insert.

ACKNOWLEDGMENT

The authors thank David F. Johnson for setting up the system.

REFERENCES

[1] A. Twin, J. Brown, F. Domptail, R. Bateman, R. Harrison, M. Lakrimi, Z. Melhem, P. Noonan, M. Field, S. Hong, K. Marken, H. Miao, J. Parrell, and Y. Zhang, "Present and future applications for advanced superconducting materials in high field magnets," *IEEE Trans. Appl. Supercond.*, vol. 17, no. 2, pp. 2295–2298, June 2007.

[2] H. Lee, E. Bobrov, J. Bascuñán, S. Hahn, and Y. Iwasa, "An HTS insert for Phase 2 of a 3-Phase 1-GHz LTS/HTS NMR magnet," *IEEE Trans. Appl. Supercond.*, vol. 15, no. 2, pp. 1299–1302, June 2005.

[3] J. Bascuñán, W. Kim, S. Hahn, E. S. Bobrov, H. Lee, and Y. Iwasa, "An LTS/HTS NMR magnet operated in the range 600–700 MHz," *IEEE Trans. Appl. Supercond.*, vol. 17, no. 2, pp. 1446–1449, June 2007.

[4] S. Hahn, J. Bascuñán, W. Kim, E. S. Bobrov, H. Lee, and Y. Iwasa, "Field mapping, NMR lineshape, and screening currents induced field analyses for homogeneity improvement in LTS/HTS NMR magnets," *IEEE Trans. Appl. Supercond.*, vol. 18, no. 2, pp. 856–859, June 2008.

[5] S. Hahn, J. Bascuñán, H. Lee, E. S. Bobrov, W. Kim, M. C. Ahn, and Y. Iwasa, "Operation and performance analyses of 350- and 700-MHz LTS/HTS NMR magnet: A new class of superconducting NMR magnets targeted to reach an operating frequency of 1.3 GHz," *Journal of Applied Physics*, submitted for publication.

[6] H. Lee, J. Bascuñán, and Y. Iwasa, "A high-temperature superconducting double-pancake insert for an NMR magnet," *IEEE Trans. Appl. Supercond.*, vol. 13, no. 2, pp. 1546–1549, June 2003.

[7] M. C. Ahn, T. Yagai, S. Hahn, R. Ando, J. Bascuñán, and Y. Iwasa, "Spatial and temporal variations of a screening current induced magnetic field in a double-pancake HTS insert for NMR magnet," *IEEE Trans. Appl. Supercond.*, submitted for publication.